Author/s:
Kuribara, T;Hirano, M;Speciale, G;Williams, SJ;Ito, Y;Totani, K

Title:
Selective Manipulation of Discrete Mannosidase Activities in the Endoplasmic Reticulum by Using Reciprocally Selective Inhibitors

Date:
2017-06-01

Citation:
Kuribara, T., Hirano, M., Speciale, G., Williams, S. J., Ito, Y. & Totani, K. (2017). Selective Manipulation of Discrete Mannosidase Activities in the Endoplasmic Reticulum by Using Reciprocally Selective Inhibitors. Chembiochem, 18 (11), pp.1027-1035. https://doi.org/10.1002/cbic.201700081.

Persistent Link:
https://hdl.handle.net/11343/292863

Title: Selective Manipulation of Discrete Mannosidase Activities in the Endoplasmic Reticulum by Using Reciprocally Selective Inhibitors

Authors: Taiki Kuribara; Makoto Hirano, Ph.D.; Gaetano Speciale, Ph.D.; Spencer J. Williams, Ph.D.; Yukishige Ito, Ph.D.; Kiichiro Totani, Ph.D.

To be cited as: ChemBioChem 10.1002/cbic.201700081

Link to VoR: https://doi.org/10.1002/cbic.201700081

Selective Manipulation of Discrete Mannosidase Activities in the Endoplasmic Reticulum by Using Reciprocally Selective Inhibitors

Taiki Kuribara,[a] Makoto Hirano,[a] Gaetano Speciale,[b] Spencer J. Williams,[b] Yukishige Ito,[c] and Kiichiro Totani*[a]

Abstract: Within the endoplasmic reticulum immature glycoproteins are sorted to secretion and degradation pathways through the sequential trimming of mannose residues from $Man_9GlcNAc_2$ to $Man_5GlcNAc_2$ by the combined actions of assorted α-1,2-mannosidases. It has been speculated that specific glycoforms encode signals for secretion and degradation. However, it is unclear whether the specific signal glycoforms are produced by random mannosidase action or are produced regioselectively in a sequenced manner by specific α-1,2-mannosidases. Here we report identification of a set of selective mannosidase inhibitors and development of conditions for their use that enable production of distinct pools of $Man_8GlcNAc_2$-isomers from a structurally-defined synthetic $Man_9GlcNAc_2$-substrate in an endoplasmic reticulum fraction. Glycan processing analysis with these inhibitors provide the first biochemical evidence for selective production of the signal glycoforms contributing to traffic control in glycoprotein quality control.

Introduction

An estimated 30% of newly generated cellular proteins are terminally unfolded and proteasomally degraded.[1] Glycoprotein quality control in the endoplasmic reticulum (ER) contributes toward traffic control of secreted and degraded glycoproteins based on specific high-mannose type glycoforms, thereby maintaining cellular homeostasis.[2-4] $Man_{8B}GlcNAc_2$ (M8B), generated by trimming a mannose from the B-branch of $Man_9GlcNAc_2$ (M9), is believed to act as a secretion signal, whereas some further trimmed $Man_{5-6}GlcNAc_2$ (M5-6) isomers, possibly derived from $Man_{8A/C}GlcNAc_2$ (M8A/C), which are in turn generated from trimming the A- or C-branches of M9, are proposed to be degradation signals (Figure 1).[5] Based on ER-dependent lectin/enzyme specificity,[6] removal of a mannose from the B-branch is favorable for binding to the lectin-like cargo-receptor complex, ER-Golgi intermediate compartment 53 kDa protein (ERGIC-53)•multiple coagulation factor deficiency protein 2 (MCFD2), which is involved in secretion. In contrast, removal of a mannose from the A-branch is unfavorable for UDP-glucose: glycoprotein glucosyltransferase (UGGT) activity and vesicular integral-membrane protein of 36 kDa (VIP36)/vesicular integral-membrane protein of 36 kDa-like (VIPL) lectin binding, key events involved in protein folding and secretion. Moreover, removal of a mannose from the C-branch provides glycoproteins that preferentially bind to the lectin Osteosarcoma amplified 9 (OS-9), which is involved in degradation. Accordingly, M8A/C can also be considered degradation signals.

ER-localized α-1,2-mannosidases belonging to glycoside hydrolase family 47 (GH47) appear to be responsible for M8 production including ER mannosidase I (ERManI) and ER degradation-enhancing mannosidase-like proteins (EDEMs), namely EDEM1, EDEM2 and EDEM3. Product analysis of recombinant ERManI revealed the specific production of M8B from M9,[7,8] whereas recent reports studying the localization of ERManI revealed that this enzyme is controversially localized in the Golgi apparatus[9] or quality control vesicles.[10] On the other hand, detection of glycan trimming activities of purified EDEM1/2/3 have not been successful. Instead, their specificities have been inferred based on glycoform analysis of transgenic cell lines, with the suggestion that EDEM1 mediates mannose trimming from the A- and C-branches,[11,12] EDEM2 mediates trimming from the B-branch,[13] and EDEM3 mediates trimming with no branch specificity.[14] Taken together, these results indicate that multiple α-mannosidases act in parallel in the ER. While there is growing evidence that the specific trimmed glycan isomers are trafficking signals, little is known about how these products are formed and whether there are distinct trimming pathways leading to secretion or degradation signals. One approach to study the trimming process is to utilize an ER-derived protein mixture in which the entire processing pathway is intact, and to use selective α-1,2-mannosidase inhibitors to block individual enzyme activities. Such inhibitor based approaches provide a biochemical description for the production of signal glycoforms, while genetics based approaches are currently premature as the molecular entities responsible for the mannose-trimming pathway(s) are yet to be rigorously identified. However, despite the extensive range of glycosidase inhibitors available, their specificity for individual ER α-1,2-mannosidases

[a] T. Kuribara, Dr. M. Hirano, Dr. K. Totani
Department of Materials and Life Science
Seikei University
3-3-1 Kichijoji-kitamachi, Musashino, Tokyo 180-8633 (Japan)
E-mail: ktotani@st.seikei.ac.jp
[b] G. Speciale, Prof. Dr. S. J. Williams
School of Chemistry and Bio21 Molecular Science and Biotechnology Institute
University of Melbourne
30 Flemington Road, Parkville, VIC 3010 (Australia)
[c] Dr. Y. Ito
Synthetic Cellular Chemistry Laboratory, RIKEN, 2-1 Hirosawa, Wako, Saitama 351-0198 (Japan)

Supporting information for this article is given via a link at the end of the document.

has not been comprehensively studied and conditions allowing selective inhibition in complex mixtures have not been identified. Herein, inhibition selectivities of various iminosugars on glycan-trimming α-1,2-mannosidases are comprehensively examined. Through this analysis, we identify inhibitors selective for the ER-localized α-1,2-mannosidases that enable selective manipulation of glycosignal production and have supported the discovery of two independent mannose-trimming pathways in our cell-free ER system. Our results provide molecular evidence for regioselective production of signal glycoforms contributing to traffic control of secreted and degraded glycoproteins.

Results

Identification of selective inhibitors for the ER-localized α-1,2-mannosidases

Previously, we used a series of high-mannose type glycan derivatives assembled by total synthesis[15,16] as probes for the analysis of glycoprotein glycan processing in the ER.[17-21] For instance, the dye labeled M9-Gly-BODIPY (Figure 2A) was found to be a mimic of a glycoprotein folding intermediate,[20] and the glycan processing profile obtained when using this substrate in the ER fraction from senescence-accelerated mouse prone 6 (SAMP6)[22] liver showed almost equal production of M8A/C (degradation signals) and M8B (secretion signal).[23] For the present study, this assay system provides a convenient means to explore the ability of various glycosidase inhibitors to selectively produce isomeric M8 glycoforms. Comparison of the inhibitory effects for M8 isomer production of various glycosidase inhibitors (Figure 2B)[24-26] was achieved by using M9-Gly-BODIPY as a substrate in the enriched ER fraction, prepared by centrifugal fractionation from SAMP6 liver (Figure S1).

The following compounds were studied: mannoimidazole (ManIm) and derivatives (2-phenyl ManIm, 2-phenethyl ManIm and 2-octyl ManIm) as inhibitors for GH47 family mannosidases; mannostatin A (Man A) and swainsonine (SW) as Golgi mannosidase II inhibitors; kifunensine (Kif) and 1-deoxymannojirimycin (dMJ) as ERManI inhibitors; and dMJ derivatives (*N*-butyl dMJ and *N*-decyl dMJ) and analogues [1-deoxynojirimycin (dNJ), 1-deoxygalactonojirimycin (dGJ), 1-deoxyfuconojirimycin (dFJ)] (for structures, see Figure 2B). In most *N*-glycan processing studies, these inhibitors are usually used at high concentrations, which may obscure latent selective inhibition of individual mannosidases that may become apparent at lower inhibitor concentrations. In order to unveil such selective inhibition, production of M8A/C and M8B were studied under various concentrations of each compound (Figure 3, 4; calculation of % inhibition from HPLC, see Figure S2). Figure 3 shows examples illustrating inhibition selectivities of typical mannosidase inhibitors; the corresponding IC_{50} values are shown in Table 1. Whereas ManIm inhibited M8 production with no selectivity (Figure 3A), Kif preferentially inhibited the formation of M8B. Notably, Kif almost completely (~90%) blocked M8B production at a concentration of 0.5 μM, while the levels of M8A/C remained about 50% of the control (Figure 3B). Conversely, Man A (Figure 3C), SW (Figure 3D), and dMJ (Figure 3E) exhibited an opposite profile, selectively inhibiting M8A/C production. Among these compounds dMJ was the most potent, almost completely inhibiting M8A/C production at 5 μM, while at this concentration effects on M8B production were marginal (around 40% of the control). In summary, these results reveal that by use of carefully selected inhibitor concentrations, Kif and dMJ can provide reciprocal selective inhibition of M8B and M8A/C production. In turn these results demonstrate that discrete pathways for glycosignal production must exist that are mediated by sets of regioselective α-1,2-mannosidases.

Structure-activity relationships for ManIm and dMJ

For a better understanding of inhibitor selectivity, we explored structure-activity relationships for ManIm (Figure 3A) and dMJ (Figure 3E). Based on the hypothesis that certain ERAD α-mannosidases may have hydrophobic patches adjacent to the active site to provide recognition of hydrophobic mis-folded proteins, we explored the introduction of simple aliphatic and aromatic substituents. Although a ManIm derivative with a bulky phenyl group directly attached to the imidazole (2-phenyl ManIm) showed no inhibition (Figure 4A), 2-phenethyl ManIm (Figure 4B) and 2-octyl ManIm (Figure 4C) preferentially inhibited M8A/C production. Thus the mannosidase(s) responsible for M8A/C production appear to have selective affinity for an elongated hydrophobic 2-substitutent on the imidazole moiety. Modification of dMJ to provide *N*-butyl dMJ and *N*-decyl dMJ resulted in inhibitors with similar selectivity as dMJ but with reduced inhibitory potency (Figure 4G and 4H), indicating that simple aliphatic *N*-substituents on the dMJ scaffold have no significant influence on inhibition selectivity.

We next explored analogues of dMJ. To our surprise, a very high concentration (50 mM) of glucosidase-inhibitor dNJ, a stereoisomer of dMJ at the 2-position, resulted in almost complete inhibition of M8B production, whereas activity for M8A/C production remained over 80% (Figure 4D). Thus while not surprisingly inversion of C2 stereochemistry in the nojirimycin scaffold reduced potency towards α-mannosidases, it unexpectedly resulted in selectivity for inhibition of the mannosidase(s) that produce M8B over those that produce M8A/C. On the other hand, dGJ, the C4 epimer of dNJ, showed no detectable inhibition of any mannosidase activity (Figure 4E). Weak inhibition was seen for dFJ, which has the identical stereochemistry at C2 and C4 to dMJ, but alternative stereochemistry at C3 and C5 (Figure 4F). However, an alternative binding mode for dFJ is possible wherein this inhibitor may be rotated such that C1 and C5 of dFJ overlay with C5 and C1 of dMJ, respectively, in which case the stereotriad of C4-C3-C2 in dFJ match that of C2-C3-C4 in dMJ (Figure S5). The crystal structure of ER ManI with dMJ[27] revealed that this inhibitor adopts a 'ring-flipped' $^{1}C_{4}$ conformation when bound to the enzyme active site; a similar 'ring-flipped' $^{4}C_{1}$ conformation of dFJ, rotated as outlined above, would provide a close stereochemical match to dMJ (please note: IUPAC rules require that conformational nomenclature applied to mirror image

conformations is reversed). Overall, these results show that by careful modification of the structures of iminosugars and mannoimidazoles, good selectivity for inhibition of ER-localized α-1,2-mannosidases may be obtained.

For detailed analysis of mannose trimming in the ER, we elected to use the structurally related but inversely selective iminosugars dMJ and dNJ, in light of their selectivity and commercial availability. To ensure that these compounds are in fact acting at the active site to eliminate the possibility of allosteric inhibition, we investigated their mode of inhibition. True kinetic parameters of the target enzymes cannot be measured in this reaction system because of the presence of various glycan processing enzymes, alternative substrates and lectins that affect the apparent concentration of the substrate and the activity of the enzyme. Rates of the mannose-trimming reactions were measured in the presence of dMJ or dNJ and used to construct a Dixon plot (Figure 5).[28] The intersections of the two lines of best fit obtained at different substrate concentrations were each located in the fourth quadrant, indicating that both dMJ (K_i = 0.16 μM) and dNJ (K_i = 3 mM) are competitive inhibitors of the enzyme(s) responsible for M8 production. These results indicate that these two well-known inhibitors have previously unappreciated distinct affinities for different α-1,2-mannosidases in the ER, thereby enabling selective manipulation of glycosignal production in glycoprotein quality control.

Pathway analysis for traffic-signal production using the reciprocally-selective mannosidase inhibitors

Various mannose-trimmed products from M8 to M5 are generated in the ER and can be reproduced in the cell-free ER system (Figure 1B). However, signal functions of M7 to M5 are less well understood than those of M8 isomers, and it is unclear whether M7 and M6 isomers are produced through random action of ER-localized α-1,2-mannosidases or if regioselective pathways exist for their production. We analyzed mannose-trimming from M9 to M5 using M9-Gly-BODIPY as a substrate in the ER-enriched fraction, using either dMJ or dNJ as complementary selective inhibitors (Figure 6). Ultra performance liquid chromatography (UPLC; Waters) enabled separation of M8, M7 and M6 isomers that were not clearly resolved by HPLC (Figure S3). The identity of peaks for M8A/B/C were determined as reported.[29] Comparison of the three chromatograms in Figure 7 allowed deduction of the identities of each isomer of M7 and M6 as follows: the right-side peak of M7 as “M7A”, the central-peak of M7 as “M7C”, the left-side peak of M7 as “M7B”; the right-side peak of M6 as “M6”, and the left-side peak of M6 as “M6iso”.

Two main isomers for each of M8, M7 and M6 were observed without inhibitors present (Figure 6A and Figure 7, upper panel). In the presence of 5 μM dMJ, the mannose-trimming mediated by the dMJ-insensitive mannosidase activity generated M8B as almost the sole M8 product (Figure 6B). Further trimming of M8B also generated only the later eluting (right-side) peaks for both M7 and M6 isomers (Figure 6B and Figure 7, middle panel), demonstrating that the dMJ-insensitive mannosidase activity results in a sequenced mannose-trimming pathway. Conversely, in the presence of dNJ, M9 is trimmed almost exclusively to M8A by the dNJ-insensitive mannosidase activity (Figure 6C). Further trimming under these conditions yielded only the earlier eluting (left-side) peaks of the M7 and M6 isomers (Figure 6C and Figure 7, lower panel), revealing that the dNJ-insensitive mannosidase activity also mediates a sequenced mannose-trimming pathway that is distinct from that mediated by the dMJ-insensitive mannosidase activity. Incidentally, treatment with both dMJ and dNJ almost completely suppressed all mannose-trimming activities in the ER (Figure 6D), showing that the two pathways are responsible for flux of M9 to M5. Similar results were obtained in C57BL/6 mouse liver ER (Figure S4), indicating that the dual mannose-trimming pathways are conserved across these mouse strains. These results reveal that the dMJ-insensitive mannosidase(s) has a preference for initially trimming the first B-branch mannose, then the initial C-branch mannose, followed by cleavage of the initial A-branch mannose, and finally cleavage of the second A-branch mannose (Figure 9). On the other hand the dNJ-insensitive mannosidase(s) has a preference for initially trimming the first A-branch mannose, followed by the first C-branch mannose, then the second A-branch mannose, before finally trimming the first B-branch mannose.

Collectively, the studies with dNJ and dMJ clearly demonstrate an ordered transformation of M9 to specific M8, M7, M6 and M5 isomers in the presence of individual enzyme activities. However, because these assays are performed in the presence of an inhibitor of the reciprocal mannosidase, it is not clear whether products of each pathway are themselves substrates for the reciprocal mannosidase activities, and thus whether cross-over between pathways may occur. In order to probe this possibility, a suite of intermediate glycan products formed by partial digestion of M9 in the absence of inhibitors were then further digested by the cell-free ER system under blockade by dMJ or dNJ. Thus, M9-Gly-BODIPY was partially digested with the ER-enriched fraction, resulting in a mixture of M9, M8 isomers, M7 isomers, M6 isomers and M5 (Figure 8A). Next, dMJ or dNJ were added into the mixture to selectively inhibit the corresponding mannosidase activity, followed by further incubation to evaluate whether cross-over occurs between the pathways. The resulting UPLC chromatograms with dMJ (Figure 8B) and the product ratio for the M8A, M7B and M6iso isomers (Figure 8D), which are regioselectively produced by the dNJ-insensitive mannosidase activity, showed no significant changes. This indicates that the dMJ-insensitive mannosidase(s) do not act upon M8A, M7B and M6iso. On the other hand, the chromatograms obtained upon treatment of the partially digested mixture with dNJ (Figure 8C) and the product ratio for M8B, M7A and M6 (Figure 8E), which are regioselectively produced by the dMJ-insensitive mannosidase activity, showed significant consumption of M8B and generation of M6 without a change in amount of M7A. Thus M8B is a substrate for the dNJ-insensitive mannosidase(s), affording M6 via M7C through rapid transformations (Figure 9). According to the glycan profiles as shown in Figure 8C, the resulting M6 from

M7C is converted to M5 by dNJ-insensitive mannosidase(s). These results are summarized in Figure 9.

Discussion

Through the identification of inhibitors with complementary abilities to inhibit trimming mannosidases, we have for the first time demonstrated the existence of two distinct glycoprotein trimming pathways within an ER-derived cell free system. The pathway mediated by the dMJ-insensitive mannosidase(s) proceeds in the ordered sequence M9→M8B→M7A→M6→M5. On the other hand the pathway mediated by the dNJ-insensitive mannosidase(s) proceeds in the ordered sequence M9→M8A→M7B→M6iso→M5. While the products of the dNJ-insensitive mannosidase(s) are not substrates for the reciprocal enzyme activity, within the dMJ-insensitive pathway a bypass exists wherein the dNJ-insensitive mannosidase(s) can convert M8B→M7C→M6→M5, suggesting that limited cross-over between the pathways is possible.

Which enzyme(s) are responsible for each mannose-trimming pathway? Candidate ER α-1,2-mannosidases include ERManI and EDEM1/2/3. Of these, only the specificity of ERManI is well-understood, namely the ability to trim a terminal mannose from M9 to generate M8B, and the conversion of M8B to M7C.[30] Pathway analysis reveals that while the dMJ-insensitive mannosidase activity selectively forms M8B, the subsequently formed M7 isomer is M7A, which is distinct from that produced by human ERManI. Hence ERManI does not appear to be completely responsible for the observed trimming in this cell-free ER system. Mori and co-workers concluded that EDEM2 is mainly responsible for M8B generation in the ER by glycoform analysis of cell lines with gene knockout of EDEM1/2/3 or ERManI,[13] which is consistent with our inhibitor-based results. However, the specificity of EDEM2 from M8B to M5 is unknown. It is also unclear whether the dMJ-insensitive mannosidase activity is comprised of a single enzyme, or a mixture, and thus whether the observed trimming is caused exclusively by EDEM2 or whether other mannosidases are involved. Hosokawa *et al.* reported that overexpression of EDEM1 produces M7A and M6 from M8B,[12] which matches the specificity of the dMJ-insensitive mannosidase(s). Taken together, these results suggest that EDEM2 is responsible for trimming M9 to M8B, while further trimming from M8B is mediated by EDEM1.

The candidate enzyme(s) for the dNJ-insensitive mannosidase activity is less clear. Although EDEM1 appears to be capable of producing M8A,[11,12] its specificity for production of M7 isomer (M7A) from M8B differs from that observed herein of M7C in the bypass mediated by the dNJ-insensitive mannosidase(s) (Figure 9). Mori and co-workers proposed that EDEM3 may be responsible for the pathway M8B to M7A, M6 and M5.[13] Because the specificity of EDEM3 has not been fully resolved, this enzyme may be a candidate for the observed activity. On the other hand, similar specificity to the dNJ-insensitive mannosidase activity has been seen for Golgi mannosidase IA. This enzyme sequentially generates M8A, M7B, M6iso and M5 from M9,[31] a specificity identical to that of our observations. However, subtle differences in specificity exist: while Golgi mannosidase IA is reported to generate equal amount of M7A and M7C from M8B, the dNJ-insensitive activity results in only traces of M7A from M8B. Moreover, western blot analysis shows that the enriched ER fraction contains only a trace amount of Golgi mannosidase IA (Figure S1); therefore this enzyme is an unlikely candidate for the dNJ-insensitive trimming.

The discovery of the two mannose trimming pathways raises a question as to whether the glycoforms produced within these pathways play active roles in influencing glycoprotein fate in the ER. Since the starting M9-glycoproteins are substrates for UGGT,[17] which plays an important role in accelerating folding, M9-glycoproteins will be retained in the ER. Conversely, UGGT has no affinity for the M8A glycoforms generated by the dNJ-insensitive mannosidase(s), resulting in their release from the calnexin/calreticulin folding complex. Moreover, the further trimmed M7B glycoform shows significant affinity to the lectin OS9,[32] which is involved in degradation. Taken together, the mannose-trimming pathway mediated by the dNJ-insensitive mannosidase(s) would appear to be involved in glycoprotein degradation. On the other hand, M8B generated by the dMJ-insensitive mannosidase(s) shows affinity for the cargo receptor ERGIC-53•MCFD2, which is involved in secretion.[33] The M8B trimmed product M7A has a two-fold higher affinity for the cargo receptor VIPL (K_a = 2.5 × 10^4 M^{-1})[34] than for OS-9 (K_a = 1.2 × 10^4 M^{-1})[32]; hence, this trimming pathway may be considered to be involved in glycoprotein secretion.

Conclusions

Using a chemically-synthesized artificial *N*-glycan, we have identified a series of selective ER α-1,2-mannosidase inhibitors, exemplified by the readily-available iminosugars dMJ and dNJ, and defined appropriate conditions for their use in allowing the selective production of M8A and M8B in a mouse liver fraction. This technology has been used to discover the possibility of two independent trimming pathways that regioselectively produce different isomers of M8, M7 and M6 in the ER. These pathways appear to be mediated by two or more mannosidases, most likely EDEMs, having inverse sensitivity to inhibition by dMJ and dNJ. These results provide molecular evidence for regioselective production of the ER signal glycoforms, and strongly support the notion that the specific glycoforms play important roles for traffic control of glycoprotein secretion and degradation.[2-4] Our discovery that readily available iminosugars are selective ER α-1,2-mannosidase inhibitors that produce discrete pools of mannosylated *N*-glycans provides a valuable technology that will assist in understanding the glycosignals important for glycoprotein fate in the ER and other unsolved issues in glycoprotein quality control. As many protein folding diseases are known to result from malfunction of glycoprotein quality control,[35] our inhibitor-based manipulation of glycosignal structure may provide a prototype of highly specific approach to perturb and study ER stress.

Experimental Section

Materials: Reagents and solvents were purchased from standard suppliers and used without further purification. SAMP6 livers and C57BL/6 mouse livers were purchased from Sankyo Labo Service Co. Inc. (Tokyo, Japan). **Kif**, **SW**, **Man A**, **dMJ** and **dNJ** were purchased from Toronto Research Chemicals, Inc. (Toronto, Canada). **dGJ**, Anti-EDEM1 (E8406), Anti-EDEM2 (E1782) and Anti-EDEM3 (E0409) antibodies were purchased from Sigma-Aldrich Chemical Co. (MO, USA). **dFJ** and Anti-ERManI antibody (sc-104975) were purchased from Santa Cruz Biotechnology, Inc. (CA, USA). Anti-GM130 (610822) antibody was obtained from BD Biosciences (CA, USA). **M9-Gly-BODIPY**[21], **ManIm**,[36] **2-phenethyl ManIm**,[37] and ***N*-butyl dMJ**[38] were synthesized according to the literature. Chemical synthesis of ***N*-decyl dMJ**, **2-phenyl ManIm** and **2-octyl ManIm** were represented in Supporting information. HPLC was performed on a JASCO (Tokyo, Japan) LC-2000 with TSK-GEL Amide-80 column (3 μm, 4.6 mmϕ × 150 mm) from Tosoh Co. (Tokyo, Japan). UPLC was performed on a Waters (MA, USA) ACQUITY UPLC H-Class with ACQUITY UPLC Glycan BEH Amide column (1.7 μm, 2.1 mmϕ × 150 mm) from Waters.

Extraction of endoplasmic reticulum (ER) fraction: ER pellets were extracted from SAMP6 mouse (8-week-old, male) or C57BL/6 mouse (8-week-old, male) livers by centrifugal fractionation.[21] The mouse liver (0.3 g) was suspended in extraction buffer (1.2 mL) [0.25 M sucrose, 2 mM EDTA, 10 mM HEPES (pH 7.4), EDTA-free protease inhibitor cocktail 1 tablet/50 mL (Roche)]. The suspension was crushed in a motor-driven tight fitting glass/Teflon Potter Elvehjem homogenizer (20 strokes, 4 °C). The resulting smooth suspension was centrifuged (900 × *g*) at 4 °C for 10 min. The recovered supernatant was then centrifuged (5,000 × *g*) at 4 °C for 10 min. Subsequently, the recovered supernatant was centrifuged (8,000 × *g*) at 4 °C for 10 min. The recovered supernatant was centrifuged (20,000 × *g*) at 4 °C for 120 min. Finally, the pellet was collected as the ER fraction. The pellet was dissolved with solubilization buffer (100 μL per 10 mg of the pellet) [0.25 M sucrose, 2 mM EDTA, 10 mM HEPES (pH 7.4), EDTA-free protease inhibitor cocktail 1 tablet/50 mL (Roche), 1% TritonX-100]. The mixture was incubated at 4 °C for 2 h, with homogenized using pestle homogenizer in every thirty minutes to provide the ER fraction. Protein concentration of each fraction was determined using the bicinchoninic acid (BCA) protein assay Kit (Thermo). Purity of each fraction and the presence of the previously reported ER mannosidases in each fraction were analyzed by western blotting.

Western blot analysis: Each protein mixture (20 μL) was added to 5 × SDS-PAGE sample buffer (4 μL) (250 mM Tris/HCl (pH 6.8), 375 mM DTT, 10% SDS, 50% glycerol, 0.1% bromophenol blue) and boiled at 100 °C for 5 min. The treated protein samples were centrifuged (15,000 × *g*) for 3 min. The resulting each supernatant was analyzed by SDS-PAGE (3-7.5% gradient gel for anti-GM130 antibody and 7.5% gel for other antibodies), followed by transferring to PVDF membranes by transblotter for 45 min (2 mA/cm^2 for PVDF membrane surface area). The transferred membranes were soaked in blocking buffer (Blocking one / Nacalai tesque) with gentle shaking for 1 h. After removal of the blocking buffer, the membranes were incubated with primary antibody solution (Anti-BiP, Anti-GM130 Anti-ERManI, Anti-EDEM1, Anti-EDEM2, Anti-EDEM3 and Anti-GolgiManIA antibodies) with gently shaking for 16 h. After washing of membrane by TBS-T for 10 min × 3, the membranes were incubated with HRP-labeled secondary antibody solution (Anti-Rabbit IgG (Goat), or Anti-Mouse IgG (H+L), or protein G) with gently shaking for 30 min. Finally, the membranes were washed by TBS-T for 10 min × 3, followed by infiltration of chemiluminescent reagent (Immobilon Western, Millipore) to the membrane to give detectable band of the target protein analyzed by image analyzer (FluoroChemQ, ProteinSimple) (see Figure S1).

Inhibitory assay of mannosidases in the ER fraction: Reaction mixtures (20 μL for inhibitor selectivity measurement, 5 μL for inhibition mode assay) contained 60 μg and 15 μg ER proteins, 0.6% TritonX-100, 10 mM $CaCl_2$, 10 mM HEPES (pH7.4), inhibitor (for inhibition selectivity) [dMJ (0.01~100 μM), Kif (0.01~1 μM), Man A (10~5,000 μM) SW (0.01~1,000 μM), dNJ (100~50,000 μM), dGJ (10~10,000 μM), dFJ (10~50,000 μM), ManIm (10~10,000 μM), 2-phenyl ManIm (0.01~1,000 μM), 2-phenethyl ManIm (100~10,000 μM), 2-octyl ManIm (100~10,000 μM), *N*-butyl dMJ (0.1~100 μM) or *N*-decyl dMJ (10~1,000 μM)] or inhibitor (for inhibition mode assay) [dMJ (0.1, 0.2, 0.5 μM or dNJ (1,000, 3,000, 5,000 μM)). After 30 min pre-incubation at 4 °C, 2.5 μM M9-Gly-BODIPY was added to the reaction mixture. After 30 min incubation at 37 °C, CH_3CN (100 μL for inhibition selectivity, 25 μL for inhibition mode assay) was added into the reaction mixture to stop the enzyme reaction. After centrifugation (20,000 × *g*) of samples at 4 °C for 20 min, the individual supernatants (30 μL) were analyzed by HPLC [Tosoh TSK-gel Amide-80 3 μm column (4.6 mmϕ × 15 cm), mobile phase CH_3CN / 100 mM NH_4HCO_2 (pH 4.5), linear gradient from 65:35 to 50:50 over 50 min, flow rate 1.0 mL/min at 40 °C, detection: excitation, 504 nm, emission, 514 nm]. Peak areas of M8B and M8A/C were calculated using the Origin 2015 software. The area was deconvoluted from overlapping peaks using Origin 2015 deconvolution command. Examples of deconvoluted data are shown in Figure S2.

ER mannose trimming analysis with the selective inhibitors: Reaction mixtures (20 μL for SAMP6, 40 μL for C57BL/6) contained 60 μg ER proteins, 0.6% TritonX-100, 10 mM $CaCl_2$, 10 mM HEPES (pH7.4), inhibitor [dMJ (5 μM) or dNJ (50 mM)]. After pre-incubation at 4 °C for 30 min, M9-Gly-BODIPY (2.5 μM for SAMP6, 1.25 μM for C57BL/6) was added to the reaction mixture. After incubation (SAMP6: 8 h for "none", 24 h for "dMJ and dNJ", C57BL/6: 6 h for "none", 24 h for "dMJ' and "dNJ") at 37 °C, CH_3CN (100 μL for SAMP6, 200 μL for C57BL/6) was added into the reaction mixture to stop the enzyme reaction. After centrifugation (20,000 × *g*) of samples at 4 °C for 20 min, the individual supernatants were concentrated *in vacuo*. The residue was dissolved in 10 μL H_2O. Each sample was analyzed by UPLC [Waters ACQUITY UPLC Glycan BEH Amide column (1.7 μm, 2.1 mmϕ × 15 cm), mobile phase CH_3CN / 50 mM NH_4HCO_3 (pH 4.5), linear gradient from 27:73 to 35.5:65.5 over 45 min, flow rate 0.2 mL/min at 60 °C, detection: excitation, 504 nm, emission, 514 nm].

ER mannose trimming analysis with the selective inhibitors starting from the glycan mixtures: Reaction mixtures (90 μL) contained 135 μg ER proteins, 0.6% TritonX-100, 10 mM $CaCl_2$, 10 mM HEPES (pH7.4), 2.5 μM M9-Gly-BODIPY. After incubation at 37 °C for 3 h, inhibitor(s) [dMJ (5 μM) or dNJ (50 mM)] were added to the reaction mixture. After incubation at 37 °C for 3 or 12 h, the enzyme reaction was stopped and analyzed ER mannose trimming by UPLC as described above.

Acknowledgements

This work was funded by JSPS KAKENHI to K.T. (Nos. 25560420 and JP16K01938), JSPS KAKENHI to Y.I. (No. JP16H06290), a Discovery Project and Future Fellowship from the Australian Research Council to S.J.W. (Nos. DP160100597 and FT130100103) and JGC-S Scholarship Foundation to M.H.

Keywords: enzymes • glycoprotein • inhibitors • protein folding • protein transport

[1] U. Schubert, L. C. Antón, J. Gibbs, C. C. Norbury, J. W. Yewdell, J. R. Bennink, *Nature* **2000**, *404*, 770-774.

[2] J. J. Caramelo, A. J. Parodi, *FEBS Lett.* **2015**, *22*, 3379-3387.

[3] R. Benyair, N. Ogen-Shtern, G. Z. Lederkremer, *Semin. Cell Dev. Biol.* **2015**, *41*, 99-109.

[4] M. Słomińska-Wojewdózka, K. Sandvig, *Molecules* **2015**, *20*, 9816-9846.

[5] Z. Frenkel, W. Gregory, S. Kornfeld, G. Z. Lederkremer, *J. Biol. Chem.* **2003**, *278*, 34119-34124.

[6] K. Yamamoto, *Proc. Jpn. Acad. Ser. B* **2014**, *90*, 67-82.

[7] D. S. Gonzales, K. Karaveg, A. S. Vandersall-Nairn, A. Lal, K. W. Moremen, *J. Biol. Chem.* **1999**, *274*, 21375-21386.

[8] L. O. Tremblay, A. Herscovics, *Glycobiology* **1999**, *9*, 1073-1078.

[9] S. Pan, S. Wang, B. Utama, L. Huang, N. Blok, M. K. Estes, K. W. Moremen, R. N. Sifers, *Mol. Biol. Cell* **2011**, *22*, 2810-2822.

[10] R. Benyair, N. Ogen-Shtern, N. Mazkereth, B. Shai, M. Ehrlich, G. Z. Lederkremer, *Mol. Biol. Cell* **2015**, *26*, 172-184.

[11] S. Olivari, T. Cali, K. E. Salo, P. Paganetti, L. W. Ruddock, M. Molinari, *Biochem. Biophys. Res. Commun.* **2006**, *349*, 1278-1284.

[12] N. Hosokawa, L. O. Tremblay, B. Sleno, Y. Kamiya, I. Wada, K. Nagata, K. Kato, A. Herscovics, *Glycobiology* **2010**, *20*, 567-575.

[13] S. Ninagawa, T. Okada, Y. Sumitomo, Y. Kamiya, K. Kato, S. Horimoto, T. Ishikawa, S. Takeda, T. Sakuma, T. Yamamoto, K. Mori, *J. Cell Biol.* **2014**, *206*, 347-356.

[14] K. Hirao, Y. Natsuka, T. Tamura, I. Wada, D. Morito, S. Natsuka, P. Romero, B. Sleno, L. O. Tremblay, A. Herscovics, K. Nagata, N. Hosokawa, *J. Biol. Chem.* **2006**, *281*, 9650-9658.

[15] I. Matsuo, K. Totani, A. Tatami, Y. Ito, *Tetrahedron* **2006**, *62*, 8262-8277.

[16] K. Totani, I. Matsuo, Y. Ihara, Y. Ito, *Bioorg. Med. Chem* **2006**, *14*, 5220-5229.

[17] K. Totani, Y. Ihara, I. Matsuo, H. Koshino, Y. Ito, *Angew. Chem. Int. Ed.***2005**, *44*, 7050-7054.

[18] K. Totani, Y. Ihara, I. Matsuo, Y. Ito, *J. Biol. Chem.* **2006**, *281*, 31502-31508.

[19] K. Totani, Y. Ihara, I. Matsuo, Y. Ito, *J. Am. Chem. Soc.* **2008**, *130*, 2102-2107.

[20] K. Totani, Y. Ihara, T. Tsujimoto, I. Matsuo, Y. Ito, *Biochemistry* **2009**, *48*, 2933-2940.

[21] H. Matsushima, M. Hirano, Y. Ito, K. Totani, *ChemBioChem* **2013**, *14*, 753-758.

[22] K. Takahashi, T. Tsuboyama, M. Matsushita, R. Kasai, H. Okumura, T. Yamamuro, Y. Okamoto, K. Toriyama, K. Kitagawa, T. Takeda, *Bone Miner.* **1994**, *24*, 245-255.

[23] S. Iwamoto, M. Isoyama, M. Hirano, K. Yamaya, Y. Ito, I. Matsuo, K. Totani, *Glycobiology* **2013**, *23*, 121-131.

[24] T. M. Gloster, G. J. Davies, *Org. Biomol. Chem.* **2010**, *8*, 305-320.

[25] V. H. Lillelund, H. H. Jensen, X. Liang, M. Bols, *Chem. Rev.* **2002**, *102*, 515-553.

[26] A. D. Elbein, *FASEB J.* **1991**, *5*, 3055-3065.

[27] F. Vallée, K. Karaveg, A. Herscovics, K. W. Moremen, P. L. Howell, *J. Biol. Chem.* **2000**, *275*, 41287-41298.

[28] M. Dixon, *Biochem. J.* **1953**, *55*, 170-171.

[29] A. Koizumi, I. Matsuo, M. Takatani, A. Seko, M. Hachisu, Y. Takeda, Y. Ito, *Angew. Chem. Int. Ed.* **2013**, *52*, 7426-7431.

[30] A. Herscovics, P. Romero, L. O. Tremblay, *Glycobiology* **2002**, *12*, G14-G15.

[31] A. Lal, P. Pang, S. Kalelkar, P. A. Romero, A. Herscovics, K. W. Moremen, *Glycobiology* **1998**, *8*, 981-995.

[32] K. Mikami, D. Yamaguchi, H. Tateno, D. Hu, S. Y. Qin, N. Kawasaki, M. Yamada, N. Matsumoto, J. Hirabayashi, K. Yamamoto, *Glycobiology* **2010**, *20*, 310-321.

[33] N. Kawasaki, Y. Ichikawa, I. Matsuo, K. Totani, N. Matsumoto, Y. Ito, K. Yamamoto, *Blood* **2008**, *111*, 1972-1979.

[34] Y. Kamiya, D. Kamiya, K. Yamamoto, B. Nyfeler, H. P. Hauri, K. Kato, *J. Biol. Chem.* **2008**, *283*, 1857-1861.

[35] M. Wang, R. J. Kaufman, *Nature* **2016**, *529*, 326-335.

[36] T. Granier, N. Panday, A. Vasella, *Helv. Chim. Acta* **1997**, *80*, 979-987.

[37] M. Terinek, A. Vasella, *Helv. Chim. Acta* **2003**, *86*, 3482-3509.

[38] A. L. Concia, C. Lozano, J. A. Castillo, T. Parella, J. Joglar, P. Clapés, *Chem. Eur. J.* **2009**, *15*, 3808-3816.

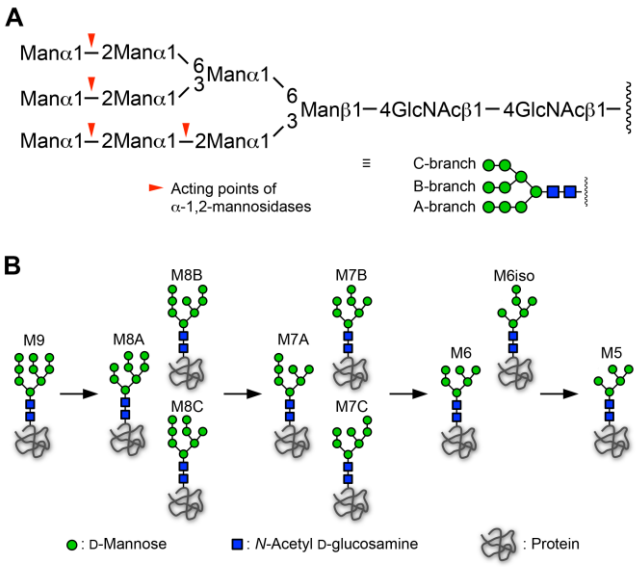

Figure 1. Mannose-trimming in ER glycoprotein quality control. A) The structure of $Man_9GlcNAc_2$ and the acting points of α-1,2-mannosidases. B) The mannose-trimming pathway in the ER.

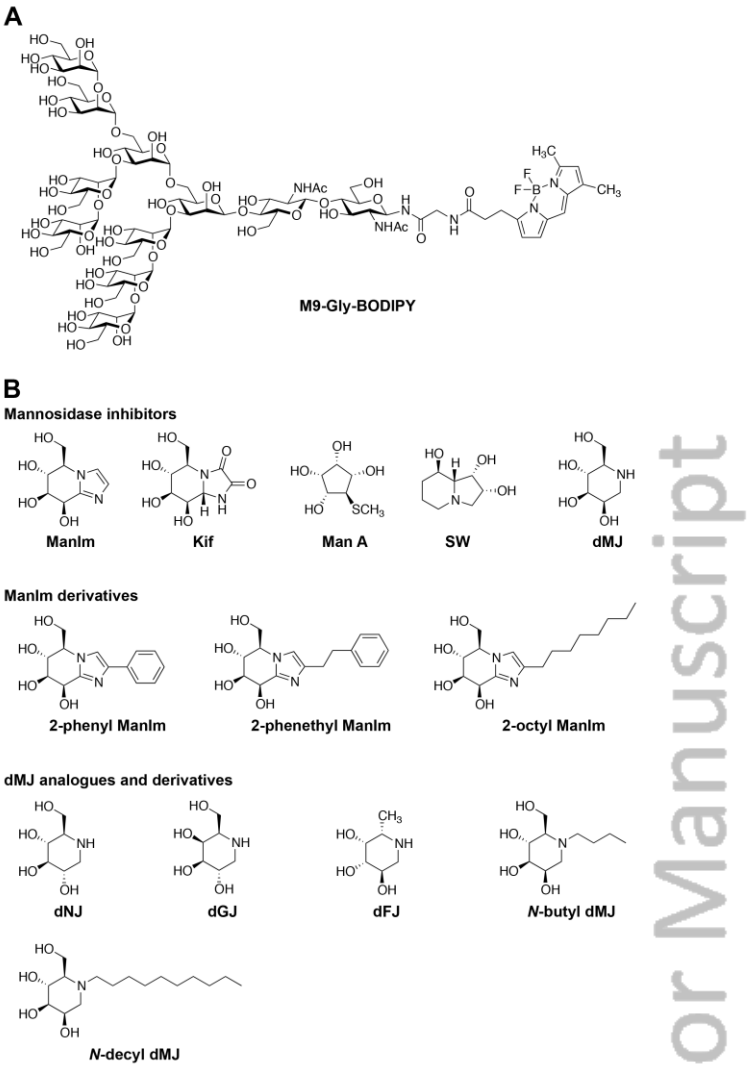

Figure 2. Structures of chemicals used in this study. A) Synthetic fluorescent substrate for the mannose trimming analysis. B) Iminosugar/cyclitol inhibitors investigated for selective signal glycoform production.

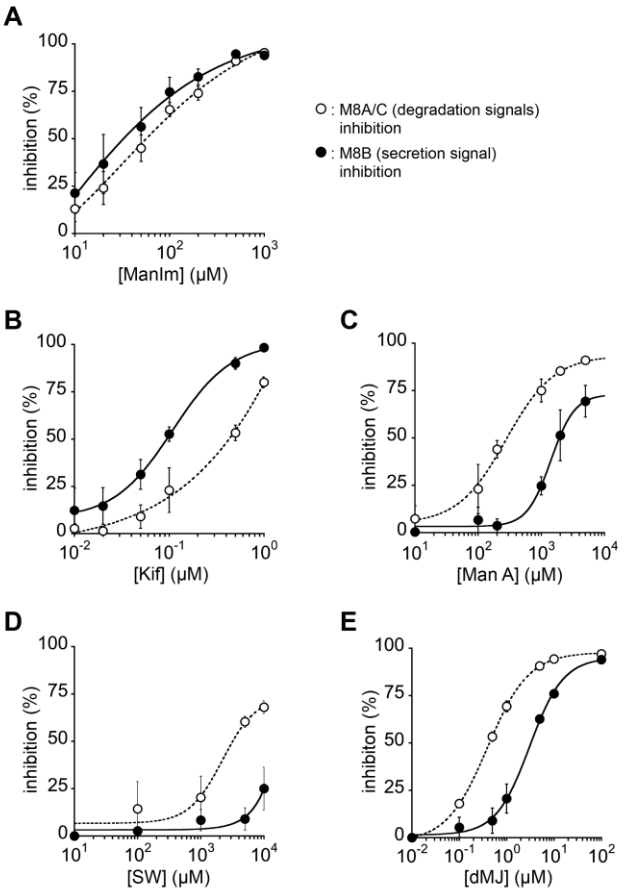

Figure 3. Inhibition selectivities of mannosidase inhibitors for production of the secretion (M8B) and degradation (M8A/C) glycosignals. Inhibition curves for ManIm (A), Kif (B), Man A (C), SW (D) and dMJ (E). Closed circle: M8B inhibition, open circle: M8A/C inhibition. Each data point represents mean values with standard error (n=3).

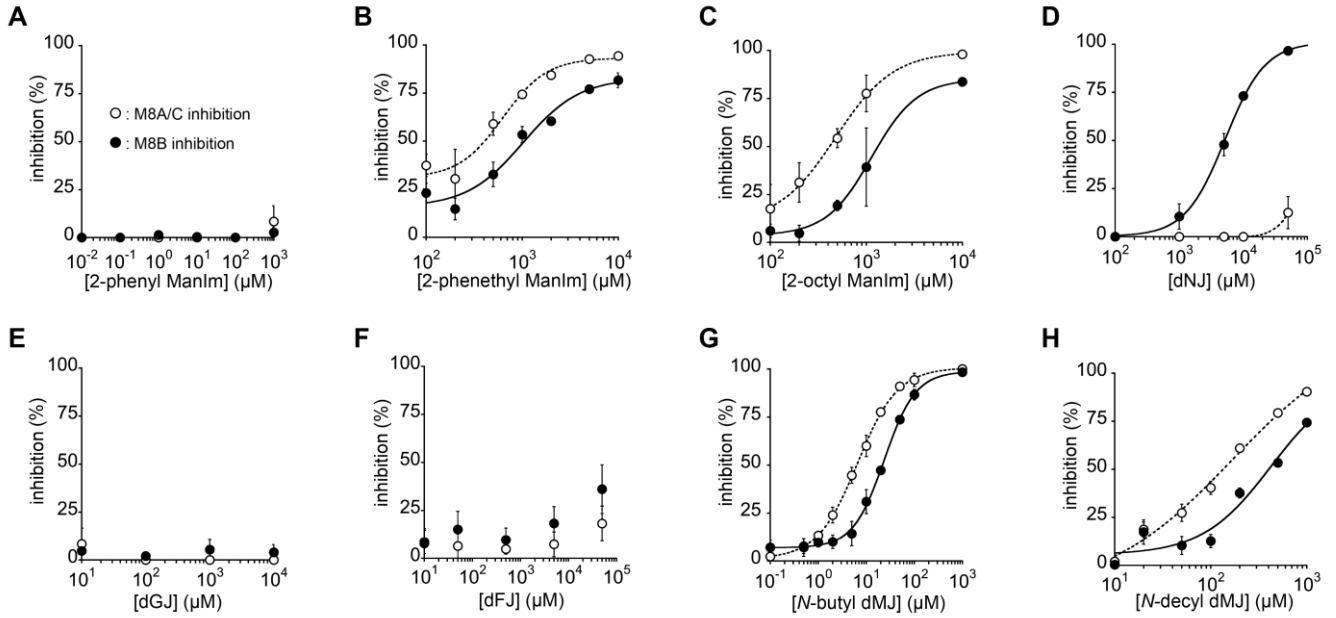

Figure 4. Inhibition selectivities of ManIm and dMJ derivatives for production of the secretion (M8B) and degradation (M8A/C) glycosignals. Inhibition curves for (A) 2-phenyl ManIm, (B) 2-phenethyl ManIm, (C) 2-octyl ManIm, (D) dNJ, (E) dGJ, (F) dFJ, (G) *N*-butyl dMJ and (H) *N*-decyl dMJ. Closed circle: M8B inhibition; open circle: M8A/C inhibition. Each data point represents mean values with standard errors (n=3).

Table 1. IC_{50} values of representative inhibitors for M8B and M8A/C production.

Inhibitor	IC_{50}^{M8B} / μM[a]	$IC_{50}^{M8A/C}$ / μM[a]
ManIm	37 ± 16	60 ± 13
Kif	0.090 ± 0.013	0.40 ± 0.080
ManA	$1.9 \times 10^3 \pm 0.66 \times 10^3$	$0.27 \times 10^3 \pm 0.090 \times 10^3$
SW	$> 1.0 \times 10^4$	$3.3 \times 10^3 \pm 0.66 \times 10^3$
dMJ	3.0 ± 0.28	0.43 ± 0.039
dNJ	$5.3 \times 10^3 \pm 0.86 \times 10^3$	$> 5.0 \times 10^4$

[a] Mean of IC_{50} values with standard error (n=3)

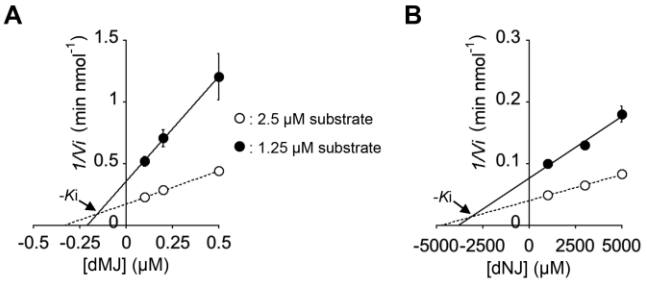

Figure 5. Determination of inhibition mode of the selective inhibitors. A) Dixon plot of dMJ in M8A/C production. B) Dixon plot of dNJ in M8B production. Closed circle: 1.25 μM substrate, open circle: 2.5 μM substrate. Each data point represents the mean values with standard errors (n=3).

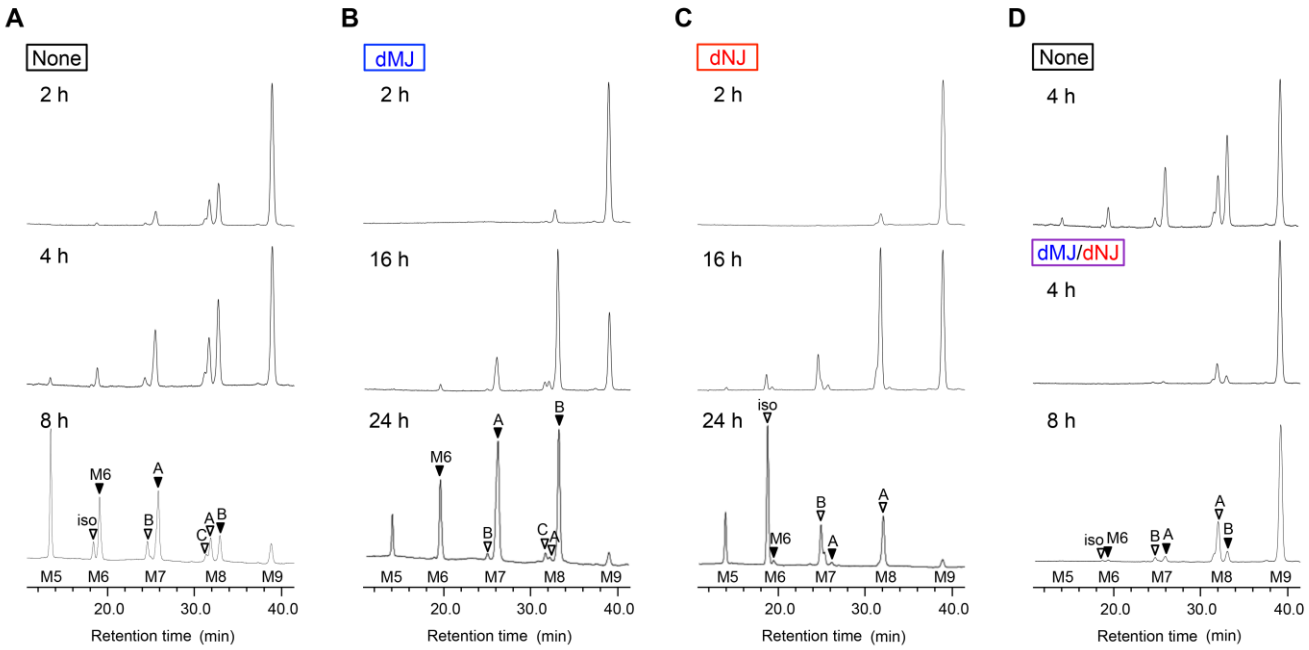

Figure 6. Time course of ER mannosidase trimming analysis with the complementary selective inhibitors. UPLC chromatograms showing mannose trimming under the conditions of (A) without inhibitors, (B) with 5 μM dMJ, (C) with 50 mM dNJ, and (D) with both 5 μM dMJ and 50 mM dNJ. UPLC conditions: Waters ACQUITY UPLC Glycan BEH Amide column (1.7 μm, 2.1 mmϕ × 15 cm), mobile phase CH_3CN / 50 mM NH_4HCO_2 (pH 4.5), linear gradient from 27:73 to 34.5:65.5 over 45 min, flow rate 0.2 mL/min at 60 °C, detection: excitation, 504 nm, emission, 514 nm.

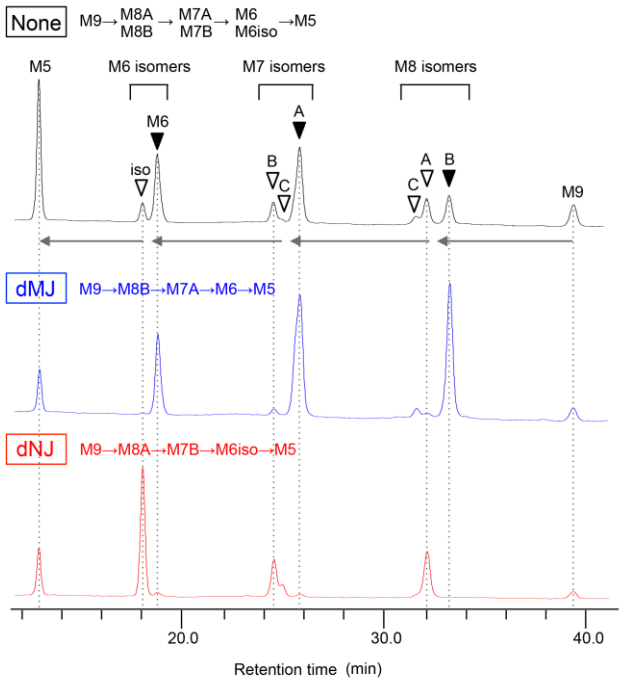

Figure 7. Typical glycan profiles for ER mannosidase trimming analysis with the complementary selective inhibitors. UPLC chromatograms showing mannose trimming in the absence or presence of dMJ, or dNJ. Reaction time; 8 h for "None", 24 h for "dMJ" and "dNJ".

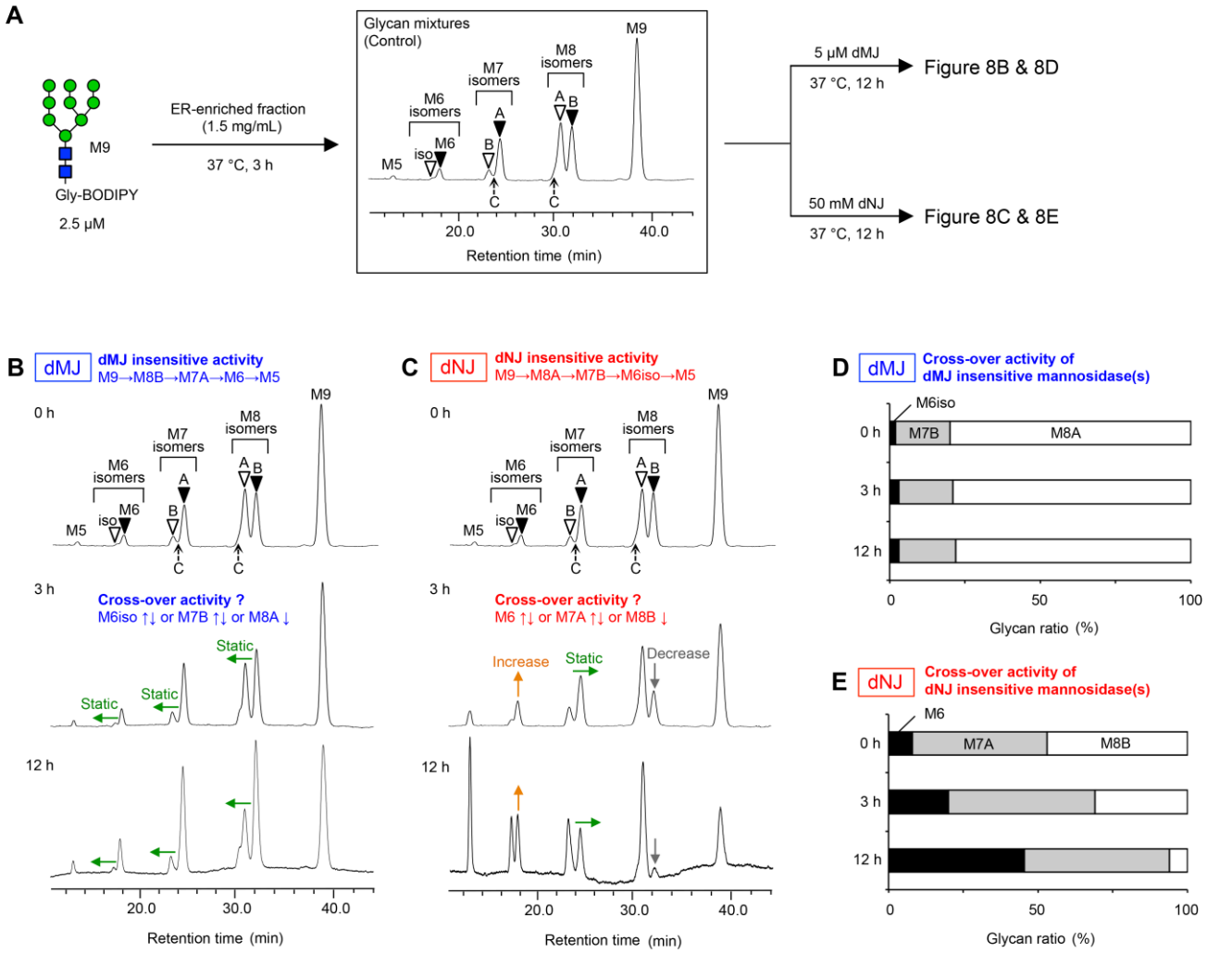

Figure 8. ER mannose trimming analysis for M9 to M5 mixtures with the complementary selective inhibitors in the ER fraction from SAMP6 liver. A) Schematic of the mannose trimming analysis starting from glycan mixtures. B) UPLC chromatograms in the presence of 5 μM dMJ. C) UPLC chromatograms in the presence of 50 mM dNJ. Glycan ratio related to the cross-over activity of mannose trimming in the presence of dMJ (D), or dNJ (E) starting from glycan mixtures.

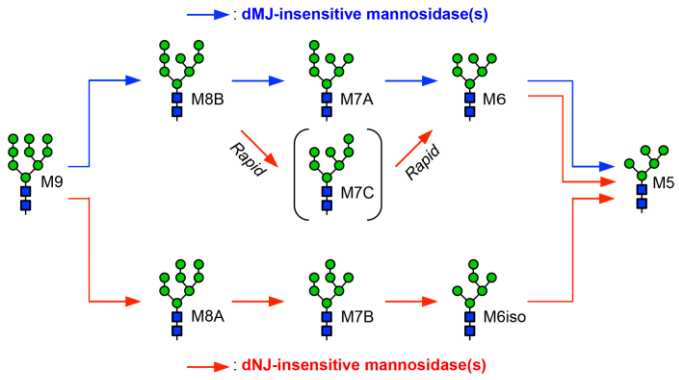

Figure 9. Observed mannose trimming pathways in the cell-free ER system.

Entry for the Table of Contents

FULL PAPER

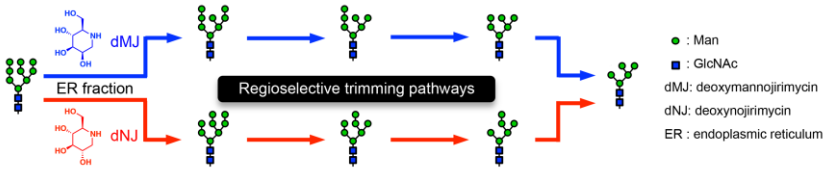

Selective inhibitors for glycoprotein quality control. We report discovery of a set of selective mannosidase inhibitors, exemplified by deoxymannojirimycin (dMJ) and deoxynojirimycin (dNJ), and conditions for their use. Glycan processing analysis with these inhibitors provided biochemical evidence for regioselective production of signal glycoforms contributing to traffic control in glycoprotein quality control.

*Taiki Kuribara, Makoto Hirano, Gaetano Speciale, Spencer J. Williams, Yukishige Ito, Kiichiro Totani**

Page No. – Page No.

Selective Manipulation of Discrete Mannosidase Activities in the Endoplasmic Reticulum by Using Reciprocally Selective Inhibitors